Synergism of *Bacillus thuringiensis* toxins by a fragment of a toxin-binding cadherin

Jiang Chen*, Gang Hua*, Juan Luis Jurat-Fuentes*†, Mohd Amir Abdullah*‡, and Michael J. Adang*§¶

Departments of *Entomology and §Biochemistry and Molecular Biology, University of Georgia, Athens, GA 30602-2603

Communicated by John H. Law, University of Georgia, Athens, GA, June 29, 2007 (received for review December 11, 2006)

The insecticidal crystal proteins produced by *Bacillus thuringiensis* (Bt) are broadly used to control insect pests with agricultural importance. The cadherin Bt-R_1 is a binding protein for Bt Cry1A toxins in midgut epithelia of tobacco hornworm (*Manduca sexta*). We previously identified the Bt-R_1 region most proximal to the cell membrane (CR12-MPED) as the essential binding region required for Cry1Ab-mediated cytotoxicity. Here, we report that a peptide containing this region expressed in *Escherichia coli* functions as a synergist of Cry1A toxicity against lepidopteran larvae. Far-UV circular dichroism and ^{1}H-NMR spectroscopy confirmed that our purified CR12-MPED peptide mainly consisted of β-strands and random coils with unfolded structure. CR12-MPED peptide bound brush border membrane vesicles with high affinity (K_d = 32 nM) and insect midgut microvilli but did not alter Cry1Ab or Cry1Ac binding localization in the midgut. By BIAcore analysis we demonstrate that Cry1Ab binds CR12-MPED at high (9 nM)- and low (1 μM)-affinity sites. CR12-MPED-mediated Cry1A toxicity enhancement was significantly reduced when the high-affinity Cry1A-binding epitope (^{1416}GVLTLNIQ^{1423}) within the peptide was altered. Because the mixtures of low Bt toxin dose and CR12-MPED peptide effectively control target insect pests, our discovery has important implications related to the use of this peptide to enhance insecticidal activity of Bt toxin-based biopesticides and transgenic Bt crops.

Cry insecticidal protein | synergist

Bacillus thuringiensis (Bt) Cry1A proteins are pore-forming toxins that are specifically toxic to insect larvae in the order Lepidoptera. This family of proteins is widely used for insect control with Bt-transgenic crops, particularly cotton, and Bt microbial pesticides. Two issues on the deployment of Bt crops are the evolution of resistance in target pests and the lower level of control of specific target pests. Although insect resistance to Bt cotton has not caused a control failure in the field, there is a natural difference in lepidopteran susceptibility that effects insect control. For example, Bt cotton expressing only a Cry1A protein is highly effective in controlling tobacco budworm (*Heliothis virescens*) populations, whereas control of cotton bollworm (*Helicoverpa zea*) larvae is only achieved after additional insecticide treatment (1).

The mode of action for Cry1A toxins includes sequential steps that determine their specificity. After ingestion by the lepidopteran larvae, Cry1A proteins are solubilized and activated to a toxic form by the insect digestive fluids. After crossing the peritrophic matrix, activated toxins bind to specific proteins on the midgut microvilli. According to a current model (2), monomeric toxin binds a cadherin, facilitating further processing necessary for toxin oligomerization. Toxin oligomers display high-affinity binding to proteins that are attached to the cell membrane by a glycosylphosphatidylinositol anchor, such as aminopeptidase or alkaline phosphatase. This binding and the localization of glycosylphosphatidylinositol-anchored proteins in specific membrane regions called lipid rafts result in oligomer insertion, formation of a pore and cell death by osmotic shock. An alternative model (3) proposes the activation of intracellular signaling pathways by toxin monomer binding to cadherin. After enterocyte death, septicemia induced by midgut bacteria leads to insect death (4).

The 210-kDa cadherin Bt-R_1 in the midgut of *Manduca sexta* larvae is a transmembrane glycoprotein containing 12 cadherin repeats (CR) and one membrane-proximal extracellular domain (MPED) in its extracellular portion (5). Unlike other members of the cadherin superfamily that localize to the intercellular adhesion points (6), Bt-R_1 is most abundant on the microvilli of midgut epithelia (7). Bt-R_1 is a high-affinity binding protein for Cry1Aa, Cry1Ab, and Cry1Ac toxins (8). Three Cry1Ab-binding regions, CR7 (9), CR11 (5), and CR12-MPED (10), have been identified on the Bt-R_1 extracellular portion. However, only the CR12-MPED fragment was reported as the functional receptor region for Cry1Ab binding and cytotoxicity (10).

Homologs of Bt-R_1 cadherin are identified as Cry1A binding proteins in other lepidopteran species, including several important agricultural pests (11–13). The loss of cadherin proteins is causally associated with target site resistance to Cry1Ac in tobacco budworm (*H. virescens*) (14). In two other species, pink bollworm (*Pectinophora gossypiella*) (15) and cotton bollworm (*Helicoverpa armigera*) (16), mutations in cadherin genes are genetically linked to Bt resistance.

The original goal of this study was to establish the relevance of the CR12-MPED fragment in Cry1Ab-intoxication. This peptide fragment was expressed and purified from *Escherichia coli* and fed with Cry1Ab toxin to *M. sexta* larvae. We expected that this peptide would block Cry1Ab binding to Bt-R_1 in the midgut, hence neutralizing Cry1Ab toxicity. However, the addition of CR12-MPED resulted in dramatically enhanced Cry1Ab-induced insect mortality. Further bioassays demonstrated that the CR12-MPED peptide could also potentiate Cry1Ac toxicity against other lepidopteran pest species, indicating that this peptide may have practical utility for insect pest control.

Results

CR12-MPED Peptide Is Structurally Unfolded. The CR12-MPED region of Bt-R_1 (Fig. 1*A*) formed inclusion bodies during expression in *E. coli*. After solubilization and purification, the resultant peptide had the expected size of 23.3 kDa on SDS/PAGE (Fig. 1*B*). Although the predicted structure of CR12-MPED based on homology modeling contains extensive β-strands (17), the far-UV circular dichroism (CD) spectra indicated the composition of

Author contributions: J.C. and G.H. contributed equally to this work; J.C., G.H., J.L.J.-F., M.A.A., and M.J.A. designed research; J.C., G.H., J.L.J.-F., and M.A.A. performed research; J.C., G.H., J.L.J.-F., M.A.A., and M.J.A. analyzed data; and J.C., G.H., J.L.J.-F., M.A.A., and M.J.A. wrote the paper.

Conflict of interest statement: J.C., G.H., M.A.A., and M.J.A. are coinventors on the U.S. patent application Peptides for Inhibiting Insects (US 20050283857). M.J.A. is a founder of InsectiGen, a start-up biotech company in Athens, GA, that is developing and commercializing this technology and is chief scientific officer of InsectiGen. M.A.A. is currently employed by InsectiGen.

Abbreviations: BBMV, brush border membrane vesicles; Bt, *Bacillus thuringiensis*; CD, circular dichroism; CR, cadherin repeats; MPED, membrane-proximal extracellular domain; TAMRA, 5-(6)-carboxyl-tetramethylrhodamine; TBR, toxin binding region.

†Present address: Department of Entomology and Plant Pathology, University of Tennessee, Knoxville, TN 37996-4560.

‡Present address: InsectiGen, Inc., 425 River Road, Athens, GA 30602-2771.

¶To whom correspondence should be addressed. E-mail: adang@uga.edu.

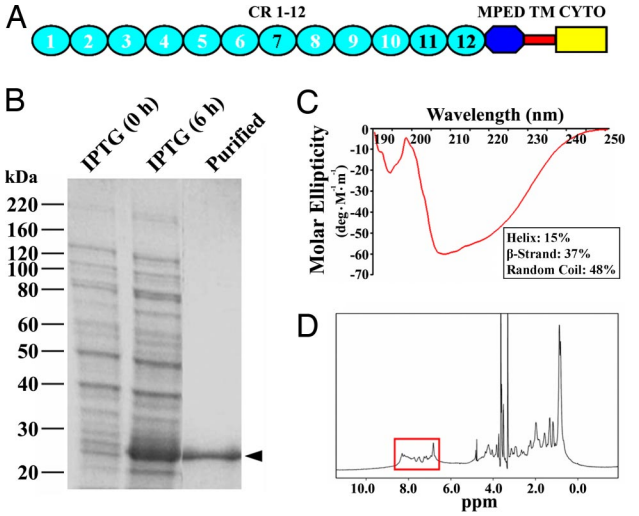

Fig. 1. Purified CR12-MPED has unfolded structure. (*A*) Structure of BtR_1 with numbers of ectodomains reported to contain Cry1Ab binding sites in black. (*B*) SDS/PAGE of lysates from *E. coli* transformed with pET-CR12-MPED before (IPTG-0h) and 6 h after induction (IPTG-6h) and purified CR12-MPED obtained from a Ni^{2+}-column. (*C*) Far-UV CD spectrum (190–250 nm) of CR12-MPED peptide, indicative of a mixture of 15% helix, 37% β-strands, and 48% random coils. (*D*) Chemical shifts of amide protons (red boxed) on CR12-MPED backbone clustered within a narrow range of ≈7–8.5 ppm in 600 MHz ^{1}H-NMR spectroscopy, evidence of the unfolded state of this peptide.

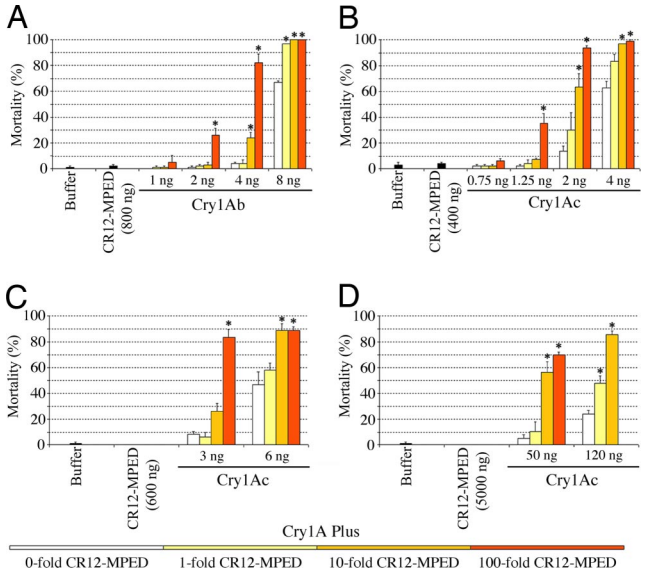

Fig. 2. CR12-MPED peptide enhances Cry1A toxicity toward lepidopteran larvae in diet surface bioassays. Cry1A toxins were mixed with purified CR12-MPED at toxin:peptide ratios of 1:0, 1:1, 1:10, and 1:100. Control treatments included buffer and CR12-MPED alone. (*A*) Cry1Ab plus CR12-MPED against *M. sexta*. (*B*) Cry1Ac plus CR12-MPED against *M. sexta*. (*C*) Cry1Ac plus CR12-MPED against *H. virescens*. (*D*) Cry1Ac plus CR12-MPED against *H. zea*. Each column presents data for the mean ± standard errors from three replicate bioassays with 32 larvae per treatment. For each species, an asterisk above the column indicates that the mortality of Cry1A plus CR12-MPED treatment showed significant difference from Cry1A alone treatment with the same Cry1A dosage (Tukey's test, $\alpha = 0.05$).

CR12-MPED was 15% helix, 37% β-strands, and 48% random coils (Fig. 1*C*). ^{1}H-NMR spectroscopy showed the chemical shifts of amide protons on the CR12-MPED backbone clustering in a narrow range of ≈7 to 8.5 ppm (Fig. 1*D*), confirming the unfolded state of this peptide after purification.

CR12-MPED Peptide Enhances Cry1A Toxicity to Lepidopteran Larvae. Because the CR12-MPED peptide contained the critical Cry1Ab-binding region (10), we predicted that this peptide would reduce the potency of Cry1Ab against *M. sexta* larvae. However, we observed a significant enhancement of Cry1Ab toxicity to *M. sexta* larvae when including CR12-MPED in our bioassays (Fig. 2*A*). This enhancing effect depended on both Cry1Ab dosage and toxin-to-peptide ratio used. For example, 4 ng/cm^2 Cry1Ab alone induced 4.2 ± 1.1% insect mortality, but when the same amount of toxin was mixed with 10 or 100-fold of CR12-MPED, larval mortality reached 23.9 ± 4.2% and 82.3 ± 6.8%, respectively. At low Cry1Ab doses (1 ng/cm^2), addition of even 100-fold CR12-MPED did not increase Cry1Ab toxicity significantly. Similar toxicity enhancement effects were observed when testing Cry1Ac toxicity toward *M. sexta* larvae in the presence of CR12-MPED (Fig. 2*B*).

Because Cry1Ac is produced in Bt transgenic cotton to control *H. virescens* and *H. zea*, we tested the synergistic effect of CR12-MPED on Cry1Ac toxicity against larvae from these species. In bioassays with *H. virescens* (Fig. 2*C*), the addition of 100-fold CR12-MPED resulted in an increase in the mortality observed with 3 ng/cm^2 of Cry1Ac from 5.2 ± 2.8% to 83.4 ± 6.3% mortality. *H. zea* is less susceptible to Cry1Ac than *H. virescens* and consequently more difficult to control with Bt transgenic cotton and sprayed Bt biopesticides (18, 19). In our bioassays (Fig. 2*D*), treatment with 120 ng/cm^2 of Cry1Ac caused 24.0 ± 2.8% *H. zea* larval mortality, whereas the addition of 1 or 10-fold excess of CR12-MPED resulted in 47.9 ± 5.5% and 85.4 ± 2.8% mortality, respectively. In controls, insecticidal activity was not observed when insects were fed with buffer or the highest CR12-MPED peptide concentration used (from 400 to 5,000 ng/cm^2) alone, evidence that Cry1Ab and Cry1Ac toxicity enhancement was due to a synergistic rather than direct effect of CR12-MPED.

Toxicity Enhancement Depends on Cry1A Binding to a Region of CR12-MPED. Xie *et al.* (20) used alanine scanning mutagenesis to map a critical Cry1A-binding region (^{1423}GVLTLNFQ^{1430}) in the cadherin HevCaLP from *H. virescens*. The homologue to this region in Bt-R_1 (^{1416}GVLTLNIQ^{1423}) is contained within CR12-MPED. A peptide derivative, CR12-MPED/Del, was constructed to remove this toxin-binding region from CR12-MPED. As shown in Fig. 3*A* (inset), ^{125}I-labeled Cry1Ab bound specifically to CR12-MPED on dot blots. In contrast, CR12-MPED/Del did not bind to the toxin, thus confirming that the removed residues in this peptide were essential determinants for toxin binding. CR12-MPED and CR12-MPED/Del were further evaluated for Cry1Ab binding by surface plasmon resonance (Fig. 3*A*). Only CR12-MPED bound Cry1Ab significantly. A model for Cry1Ab binding to CR12-MPED fits a heterologous ligand with parallel binding reactions, with one analyte, i.e., toxin, binding independently to two ligand sites on the peptide (goodness of fit, $\chi^2 = 7.26$). Toxin binding to CR12-MPED was also evaluated at different analyte concentrations followed by global fitting of all of the response curves to obtain the following apparent rate constants of the bimolecular interaction: k_{a1} (1/Ms) = $1.31 \times 10^3 \pm 1.11 \times 10^2$, and k_{d1} (1/s) = $1.6 \times 10^{-3} \pm 5.64 \times 10^{-5}$. The apparent rate constants for site 2 were k_{a2} (1/Ms) = $1.59 \times 10^5 \pm 5.91 \times 10^3$, and k_{d2} (1/s) = $1.46 \times 10^{-3} \pm 8.15 \times 10^{-5}$. Binding site 1 showed lower affinity for Cry1Ab (1.04 μM) compared with site 2 (9.17 nM). However, site 1 had higher binding capacity (R_{max} = 475 resonance units) compared with site 2 (R_{max} = 51.8 resonance units). These data suggest that Cry1Ab toxin binds and saturates site 2 before binding to site 1.

In agreement with the observed lack of CR12-MPED/Del peptide binding to Cry1Ab, this peptide did not exhibit the enhancing effect observed for CR12-MPED (Fig. 3*B*). Treatments consisted of increasing doses of Cry1Ab alone or Cry1Ab plus a constant ratio of either CR12-MPED or CR12-MPED/Del. The determined LC_{50} (95% fiducial limits) values for the treatments were Cry1Ab = 2.42

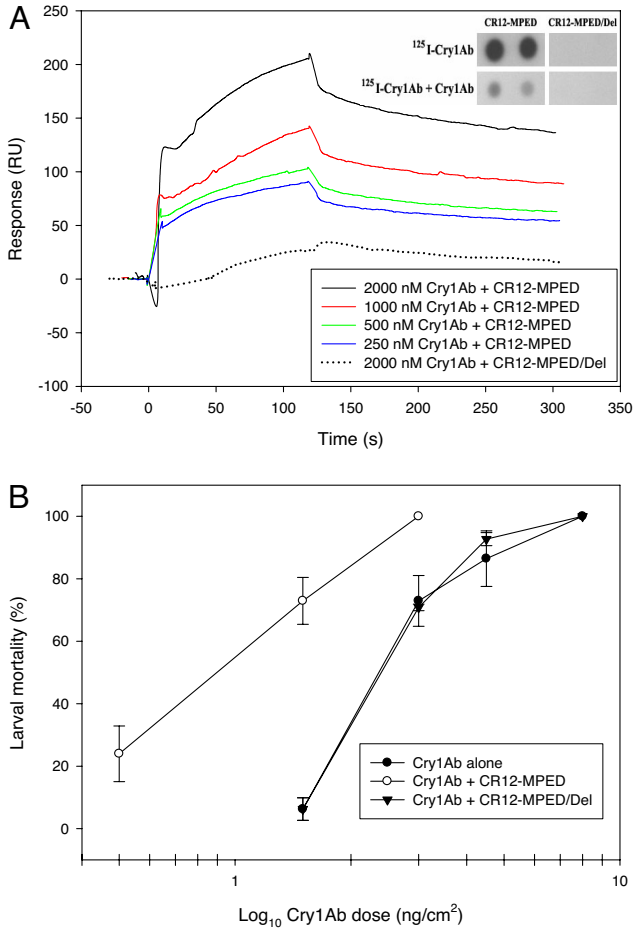

Fig. 3. Toxicity enhancement correlates with Cry1Ab binding to CR12-MPED. (*A*) Peptides were immobilized on a BIAcore chip via their C-terminal His tags. BIAcore response curves are shown for the indicated toxin concentrations. (*Inset*) CR12-MPED or CR12-MPED/Del (5 μg) were spotted in duplicate on a polyvinylidene difluoride filter and probed with ^{125}I-Cry1Ab alone or in the presence of a 1,000-fold excess of unlabeled Cry1Ab. (*B*) Cry1Ab toxicity against *M. sexta* larvae when combined with either CR12-MPED or CR12-MPED/Del at a toxin:peptide mass ratio of 1:100.

(2.21–2.64) ng/cm^2, Cry1Ab plus CR12-MPED/Del = 2.41 (2.23–2.59) ng/cm^2, and Cry1Ab plus CR12-MPED = 0.9 (0.5–1.4) ng/cm^2. These results demonstrated that CR12-MPED increased Cry1Ab toxicity ≈2.7-fold and that binding of Cry1A toxins to the ^{1416}GVLTLNIQ^{1423} region was necessary for CR12-MPED-mediated synergism.

CR12-MPED Binds Brush Border Membrane Vesicles (BBMV) Prepared from *M. sexta*. The ability of CR12-MPED to bind BBMV was tested by using ^{125}I-labeled peptide and BBMVs from *M. sexta* (Fig. 4*A*). Radiolabeled CR12-MPED bound specifically to BBMV in dot–blot binding assays. In a quantitative binding saturation assay (Fig. 4*C*), both ^{125}I-labeled CR12-MPED and CR12-MPED/Del peptides bound saturably and specifically to the membrane vesicles with calculated K_d values of 32.2 ± 5.8 nM and 27.0 ± 3.4 nM, respectively. Although CR12-MPED bound BBMV, no effects on ^{125}I-Cry1Ab or ^{125}I-Cry1Ac toxin binding was observed by using 100-fold CR12-MPED (Fig. 4*B*).

CR12-MPED Did Not Change Cry1A Binding Localization on *M. sexta* Midgut Epithelia. To test whether CR12-MPED altered the localization of Cry1A toxin binding in the larval gut epithelium, we treated midgut sections with 5-(6)-carboxyl-tetramethylrhodamine

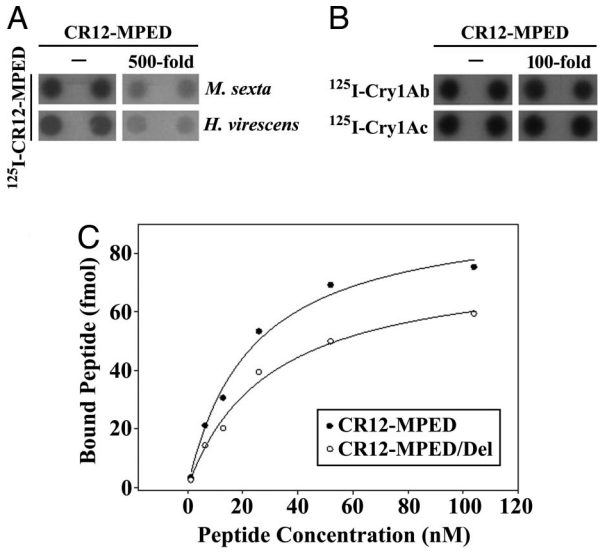

Fig. 4. CR12-MPED and CR12-MPED/Del peptides bind to BBMV. (*A* and *B*) Dot blotted *M. sexta* or *H. virescens* BBMVs (5 μg) were probed with ^{125}I-CR12-MPED (3.3 ng/ml) alone or in the presence of 500-fold unlabeled peptide (*A*), or ^{125}I-Cry1Ab or ^{125}I-Cry1Ac (3.3 ng/ml) alone or in the presence of 100-fold unlabeled CR12-MPED (*B*). (*C*) Saturation assays of ^{125}I-labeled CR12-MPED or CR12-MPED/Del binding to BBMV prepared from *M. sexta*. Data are from three experiments conducted in duplicate. Individual points are the mean amounts of peptide specifically bound-calculated after subtraction of nonspecific binding in the presence of a 500-fold excess homologous competitor from total binding.

(TAMRA)-labeled toxins. As reported in ref. 7, Cry1Ab bound to the peritrophic matrix, apical tip, and base of epithelial microvilli (Fig. 5*A*), whereas Cry1Ac bound through the entire length of microvilli (Fig. 5*D*). The addition of CR12-MPED peptide did not

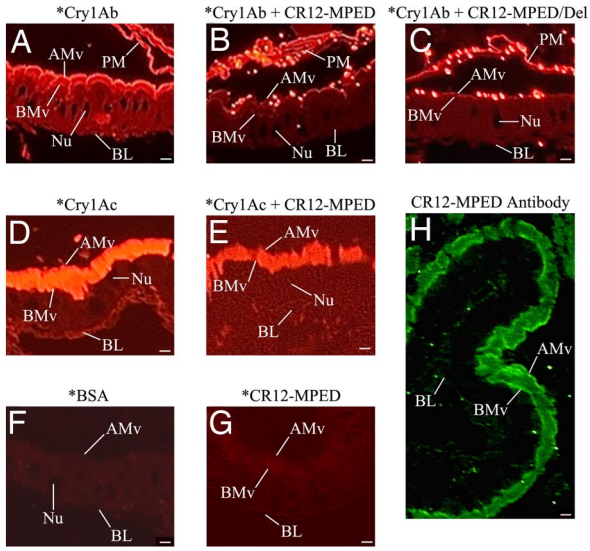

Fig. 5. Addition of CR12-MPED does not alter localization of Cry1A toxin binding in midgut sections. (*A–E*) Midgut sections were treated with TAMRA-labeled Cry1Ab (*A*) or Cry1Ac (*D*) alone or in the presence of a 20-fold excess of CR12-MPED (*B* and *E*, respectively) or CR12-MPED/Del (*C*). (*F*) Control treatment with TAMRA-labeled BSA. (*G*) Binding of TAMRA-labeled CR12-MPED. (*H*) Antiserum against CR12-MPED specifically immunostained the apex and base of microvilli. *, TAMRA-labeled; AMv, apical tip of microvilli; BL, basal lamina; BMv, base of microvilli; Nu, nucleus; PM, peritrophic matrix. (Scale bar, 10 μm.)

alter the localization of Cry1Ab binding in *M. sexta* midgut, but it induced formation of Cry1Ab aggregates that accumulated on the apical tips of microvilli and peritrophic matrix (Fig. 5*B*). However, because similar aggregates were also observed when mixing Cry1Ab with CR12-MPED/Del peptide (Fig. 5*C*), which did not potentiate Cry1Ab toxicity to *M. sexta* larvae, these Cry1Ab aggregates were probably not associated with the enhanced Cry1Ab toxicity. These aggregates were not observed when mixing 20-fold CR12-MPED and Cry1Ac (Fig. 5*E*), and only a reduction in Cry1Ac bound to microvilli was detected.

Compared with Cry1Ab and Cry1Ac, TAMRA-labeled CR12-MPED bound with low intensity to the entire length of microvilli (Fig. 5*G*). As a control, TAMRA-labeled BSA showed no binding on microvilli (Fig. 5*F*). In agreement with (7), antisera against CR12-MPED detected BtR_1 on the apex and base of midgut microvilli, (Fig. 5*H*). The ability of CR12-MPED to bind microvilli on section midgut agrees with the ^{125}I-labeled peptide and BBMV binding experiments. Binding of CR12-MPED to midgut sections and BBMV was considerably less intense than Cry1A toxin binding.

Toxin Binding Region (TBR)2 Peptide Also Enhances Cry1A Toxicity to Lepidopteran Larvae. Dorsch *et al.* (5) reported a 25-kDa Bt-R_1 truncation (TBR2), which was able to bind Cry1A toxins and completely inhibit Cry1Ab toxicity to *M. sexta* larvae. TBR2 contains the last 66 residues of CR11 (L1296 to G1362) and the first 103 residues of CR12 (I1363 to F1465). The Cry1A binding fragment (^{1416}GVLTLNIQ^{1423}) is located in CR12, which is the overlap region between TBR2 and CR12-MPED (G1362 to P1567). The TBR2 peptide contains an additional toxin-binding site in CR11 (5). When we over-expressed TBR2 following our methodology, these peptides formed inclusion bodies in *Escherichia coli*. After solubilization and purification, our TBR2 peptide bound Cry1A toxins in dot blot assays (data not shown), and in bioassays TBR2 enhanced toxicity against *M. sexta* and *H. zea* larvae. In diet bioassays against *M. sexta*, 8 ng/cm^2 Cry1Ab alone induced 16% insect mortality, but when the same amount of toxin was mixed with either 100-fold (molar ratios) of CR12-MPED or TBR2 peptide, larval mortality reached 100%. Against *H. zea*, larval mortality for Cry1Ac alone at 170 ng/ cm2 was 25%. The same amount of toxin with a 1:100 mass ratio of CR12-MPED or TBR2 induced 100% and 81% mortality, respectively.

Discussion

The cadherin Bt-R_1 serves as the primary binding protein for Cry1A toxins in *M. sexta* (2). Multiple TBRs are present on Bt-R_1, including the one located in CR12-MPED (5, 9, 10, 20). An *in vivo* approach to correlate binding with insecticidal activity for a specific TBR has been used to inhibit toxicity by mixing toxin with a Bt-R_1 truncation containing a specific TBR (5, 9, 20). The expectation is that a peptide containing a relevant toxin-binding region will inhibit toxicity by forming a Cry1A-TBR complex that blocks toxin binding to Bt-R_1 on insect microvilli. When we attempted to use this approach to validate CR12-MPED as an essential region involved in Cry1A toxicity to *M. sexta* larvae, we unexpectedly discovered that this peptide synergized Cry1A toxicity.

It is interesting that like the TBR-induced toxicity inhibition (5, 9, 20), CR12-MPED-synergized Cry1A toxicity was also relevant to toxin-peptide binding, which depended on the existence of a previously reported Cry1A-binding epitope (^{1416}GVLTLNIQ^{1423}) (20). Xie *et al.* (20) demonstrated that Cry1Ac binding to HevCaLP, a Bt-R_1 homolog in *H. virescens*, was inhibited when one of these residues was modified. In agreement with this report, CR12-MPED also lost binding to Cry1A and its synergistic ability, when the ^{1416}GVLTLNIQ^{1423} fragment was removed. These results support the correlation between Cry1A-peptide binding and synergism.

The TBR2 truncation of Bt-R1 (5) is reported to bind and completely inhibit Cry1Ab toxicity to *M. sexta* larvae. The TBR2 peptide (L1296-F1465) contains part of CR11 and CR12, overlapping with CR12-MPED (G1362-to P1567). Thus, we initially hypothesized that the enhanced Cry1Ab toxicity observed with CR12-MPED was due to the lack of additional toxin-binding sites in CR11 (5). However the TBR2 peptide we prepared from *E. coli* inclusion bodies enhanced toxicity against *M. sexta* and *H. zea* larvae as CR12-MPED.

In previous reports testing TBR2 and a fragment of HevCaLP, these peptides were purified from soluble fractions of bacterial cultures (5, 20). The TBR and CR12-MPED peptides tested in this study were extracted from inclusion bodies. Far-UV CD and ^{1}H-NMR spectroscopy demonstrated that CR12-MPED, which enhanced Cry1A activity, was an unfolded peptide with more hydrophobic residues being exposed to the surrounding environment than in a folded state. The unfolded state of CR12-MPED, with more exposed amino acid residues, may be associated with the synergistic capability to enhance Cry1A toxicity against lepidopteran larvae. It is possible that the unfolded conformation of toxin-binding cadherin fragments could modify interactions with Cry1A toxins and other molecules on insect midgut epithelium.

The CR12-MPED peptide containing the previously identified high-affinity (2.9 nM) Cry1Ab binding site (10) binds Cry1Ab toxin. In surface plasmon resonance binding experiments CR12-MPED bound Cry1Ab at high affinity (9 nM) and low affinity (1 μM) binding sites. It is possible that binding to an apparent low-affinity site was due to aggregation of CR12-MPED attached to the chip. The CR12-MPED peptide also binds to BBMV with high affinity (32 nM) and to epithelial microvilli on sectioned midgut. The nature of these interactions is unknown, but it most likely does not involve the toxin binding site, because CR12-MPED/Del also bound BBMV with high affinity (27 nM).

An explanation of the observed synergism is that CR12-MPED peptides bind to the microvilli and attract Cry1A molecules, increasing the probability of toxin interaction with Cry1A receptors, such as Bt-R_1, glycosylphosphatidylinositol-anchored aminopeptidase N (21–23) and alkaline phosphatase (22, 24, 25), or sphingoglycolipids (26). This hypothesis is consistent with the model proposed by Bravo *et al.* (2), whereby binding of Cry1A monomer to the cadherin Bt-R_1 induces structural changes in the toxin that result in further processing and formation of a toxin oligomer. As a Bt-R_1 truncation for Cry1A binding, the addition of CR12-MPED might promote the switch of toxin from monomer to oligomer, a form that primarily binds to glycosylphosphatidylinositol-anchored receptors resulting in oligomer insertion in the cell membrane (27).

An alternative explanation for toxicity enhancement is that CR12-MPED modifies the pathological site of Cry1A toxins. However, according to microscopic observations, no significant differences in pathology were detected along the alimentary channel of *M. sexta* larvae that were fed Cry1Ab alone or the mixture of Cry1Ab with CR12-MPED peptides (J.C., G.H., and M.J.A., unpublished data).

The use of synergists has become one of the methods to increase Bt Cry toxicity and to overcome and delay insect resistance to this biopesticide (28, 29). The CR12-MPED peptide is the first Cry-synergist originating from an insect protein. This peptide is able to enhance Cry1A toxicity against lepidopteran pests in diet overlay bioassays. Other Cry protein synergists have been reported, and can be categorized according to their synergistic mechanisms, including (*i*) improvement of toxin docking and membrane insertion (30, 31), (*ii*) destruction of midgut peritrophic matrix to increase toxin permeability (32, 33), and (*iii*) disruption of midgut bacterial community, which is essential for insect growth and development (4). As a synergist, CR12-MPED may accumulate on midgut microvilli, and its mediated toxicity enhancement relates to synergist-toxin binding. Although the synergistic mechanism of CR12-MPED is not fully characterized, it seems that this peptide could be grouped in the first synergist category. Another member in this category, Cyt1Aa (produced by Bt var. *israelensis*), synergizes Cry11Aa toxicity against yellow fever mosquito (*Aedes aegypti*)

larvae by functioning as a binding site and increasing toxin binding and insertion into midgut cells (31). Cyt1Aa is a cytolysin that is highly toxic not only to mosquito larvae but also to other vertebrate and invertebrate cells (34). In comparison, insects were healthy after fed CR12-MPED alone, suggesting that CR12-MPED may be used as an environmentally safe Cry1A synergist.

In summary, as a Bt Cry1A synergist, CR12-MPED peptide has the potential to augment the control of lepidopteran pests by Cry1A toxins. This synergist is a good candidate for development of a more effective strategy to control lepidopteran pests that are currently not being efficiently controlled by Bt crops, such as the case of *H. zea*. The activity of this synergist toward other insect groups and organisms needs to be established. Because homologues of Bt-R_1 cadherin are present in other lepidopteran species, it is likely that CR12-MPED may also enhance Cry1A toxicity toward alternative lepidopteran pests.

Materials and Methods

Preparation of Bt Cry1A Toxins. Growth of bacterial strains and purification and activation of Cry1Ab and Cry1Ac were as described in ref. 35. Purified toxin samples (as determined by SDS/10% PAGE) were pooled, quantified (36), and stored at −80°C.

Cloning, Expression and Purification of *M. sexta* CR12-MPED and TBR2 Peptides. Cloning of the cadherin Bt-R_1 (GenBank accession no. AY094541) from *M. sexta* larvae is described in ref. 37. The cDNA encoding Bt-R_1 cloned in the pIZT vector (Invitrogen, Carlsbad, CA) was used as template for subcloning the CR12-MPED fragment (amino acids G1362 to P1567) by PCR with primers: 5′-GTAC*CATATG*GGGATATCCACAGCGGACTCCATCG-3′ and 5′-GGCT*CTCGAG*AGGCGCCGAGTCCGGGCTGGAGTTG-3′. The TBR2 truncation (amino acids G1296 to F1465) of BtR_1 described by Dorsch *et al.* (5) was also subcloned by PCR with primers: 5′-AAAA*CATATG*CTGGATCCTGTTCGCAACAGGTTGT-3′ and 5′-AAAA*CTCGAG*CACGAAGTAGACGCGGTTCTGCGAGGAT-3′. The resulting PCR fragments were gel purified, digested by NdeI and XhoI endonucleases, and then subcloned into the pET-30a (+) vector (Novagen, Madison, WI) to yield plasmids pET-CR12-MPED and pET-TBR2, respectively. The coding sequences and clone orientation were confirmed by sequencing. The pET^- constructs were transformed into *E. coli* strain BL21(DE3)/pRIL (Stratagene, La Jolla, CA), and positive clones were selected on LB plates containing kanamycin and chloramphenicol. The CR12-MPED and TBR2 peptides were overexpressed in *E. coli* as inclusion bodies. Inclusion bodies were solublize and proteins purified on a HiTrap Ni^{2+}-chelating HP column (GE Healthcare, Piscataway, NJ). Purified proteins were dialyzed against 10 mM Tris·HCl, pH 8.0 at 4°C. Protein concentration was quantified by the method of Bradford (36) with BSA as standard. Purified CR12-MPED and TBR2 peptides were stored at −20°C. Polyclonal antisera against purified CR12-MPED were produced in New Zealand White rabbits at the Animal Resources Facility of the University of Georgia.

Deletion of Cry1A-Binding Epitope in CR12-MPED. To delete the putative Cry1A-binding epitope ^{1416}GVLTLNIQ^{1423} within the CR12-MPED peptide (20), a pair of primers containing EcoRI cleavage sites (italicized) were designed, 5′-TAAT*GAATTC*-CCCACGGCCACGATGCATGGAC-3′ and 5′-TCAG*GAATTC*GGTTTGAGCGTTCAGTACGAAAGCCG-3′. PCR was performed by using the Expand High Fidelity PCR System kit (Roche Diagnostics, Indianapolis, IN) with pET-CR12-MPED as template. The amplicon was gel-purified, digested with EcoRI, cloned into the pET-30a (+) vector and expressed as described for CR12-MPED. The expressed peptide, CR12-MPED/Del, lacked the ^{1416}GVLTLNIQ^{1423} Cry1A-binding epitope (20). These 8 aa were replaced with E and L because of the introduced EcoRI sites in the DNA sequence. Purification of CR12-MPED/Del was as described above for CR12-MPED.

Insect Bioassays. Cry1Ab or Cry1Ac was mixed with CR12-MPED at different toxin:peptide mass ratios (1:0, 1:1, 1:10, and 1:100) in buffer D. The maximum dose of CR12-MPED peptide applied with toxin was used alone in buffer D as a negative control. Toxin and peptide samples were overlaid on bioassay tray wells filled with 1 ml of artificial diet (Southland Products, Lake Village, AR). After drying, insect neonates were placed on the wells and reared at 28°C with a 12L:12D photoperiod. Bioassays were repeated thrice for each treatment, and each replicate contained 32 larvae. Larval mortality was quantified after 7 days. Data were analyzed by the GLM method and Tukey's test at $\alpha = 0.05$ nominal criterion level, using SAS 9.1 (SAS Institute, Cary, NC).

Bioassays with toxin and toxin:TBR2 peptide combinations tested against *H. zea* were conducted twice for each treatment, and each replicate contained 16 larvae. Tests with toxin and toxin:TBR2 against *M. sexta* were conducted with 32 larvae per treatment. Toxin alone and buffer controls were included with each larval bioassay. Other bioassay conditions were as described above.

To compare the bioactivity between CR12-MPED and CR12-MPED/Del, *M. sexta* neonates were fed Cry1Ab, or Cry1Ab plus 100-fold (mass) CR12-MPED or CR12-MPED/Del peptides. Bioassays were performed as described above. The LC_{50} values were calculated by Probit analysis in Softtox, version 1.1 (WindowChem, Fairfield, CA).

CD and NMR Spectroscopy. Purified CR12-MPED peptide was prepared in 10 mM Tris·HCl, pH 8.0, at a concentration of 15 μM. CD spectra were recorded with a J-815 instrument (JASCOM, Easton, MD). Data points were collected in far-UV wavelength (190–250 nm), using a 0.1-cm path length quartz cuvette at room temperature. The acquired CD spectroscopic data were analyzed by CDSSTR program (38, 39) on DICHROWEB (www.cryst.bbk.ac.uk/cdweb/html/home.html).

For ^{1}H-NMR spectroscopy, purified CR12-MPED peptide was concentrated to 0.2 mM in 1 mM Tris·HCl buffer, pH 8.0, containing 8% D_2O. Spectra were acquired at 25°C, using an INOVA 600 MHz spectrometer (Varian, Palo Alto, CA).

Labeling of Cry1A Toxins and CR12-MPED Peptide. For BBMV binding assays Cry1Ab (5 μg), or peptide (CR12-MPED or CR12-MPED/Del; 10 μg) were radiolabeled with 0.5 mCi of $Na^{125}I$, using the chloramine-T method (40) and stored at 4°C. Specific activity was 100 μCi/μg or 50 μCi/μg based on input toxin or peptides, respectively.

For histomicroscopy, Cry1Ab, Cry1Ac, CR12-MPED, or BSA (1 μg) were labeled with the rhodamine derivative TAMRA and free label separated from protein by size exclusion chromatography with Sephadex G-50 (Sigma, St. Louis, MO) as described in ref. 41. Labeled proteins were stored at −80°C.

BBMV Preparation and Binding Assay. Vesicle binding assays were conducted by using BBMV prepared from *M. sexta* midguts dissected from second-day fifth-instar larvae. Midguts were stored at −80°C, until they were used to prepare BBMV. BBMV were prepared according to (42) and stored at −80°C in 300 mM mannitol, 5 mM EGTA, 17 mM Tris, pH 7.5, until needed. BBMV proteins were quantified as for purified toxins.

For peptide binding assays, BBMV (5 μg) were incubated in 0.3 ml of binding buffer (50 mM Tris·HCl, pH 7.4/0.1 M NaCl/0.1% BSA) containing increasing amounts of ^{125}I-labeled peptide with or without 500-fold unlabeled peptide. After incubation for 60 min at room temperature, the samples were centrifuged at 13,000 × *g* for 10 min, and pellets were washed twice with 1 ml of binding buffer. Radioactivity was measured with a Beckman model Gamma 4000

counter (Beckman Coulter, Fullerton, CA). Each binding assay was repeated 3 times in duplicate.

Dot–Blot Binding Assays. CR12-MPED or CR12-MPED/Del peptide (1 μg) was dotted onto a polyvinylidene difluoride filter (Millipore, Bedford, MA). After blocking in PBS-T buffer (0.1% Tween 20 in PBS, pH 7.4) with 3% BSA, filters were bathed in 3.3 ng/ml ^{125}I-Cry1Ab or ^{125}I-Cry1Ac for 1 h at room temperature. Unlabeled Cry1Ab or Cry1Ac (1,000-fold excess) were used in competition assays. After washing off the unbound ^{125}I-labeled toxins, bound toxins were detected by autoradiography at −80°C overnight.

For dot–blot experiments with BBMV, 10 μg of *M. sexta* or *H. virescens* BBMV were spotted onto a polyvinylidene difluoride filter. After blocking as above, filters were probed with ^{125}I-CR12-MPED (3.3 ng/ml) for 2 h at room temperature. Competition assays were performed by the addition of 500-fold unlabeled CR12-MPED. After washing, bound ^{125}I-CR12-MPED was detected by autoradiography at −80°C for 3 days.

To study the effect of CR12-MPED on Cry1A toxin binding to M. sexta BBMV, 5 μg of BBMV proteins were dotted on polyvinylidene difluoride filters. After blocking, filters were probed with 3.3 ng/ml ^{125}I-Cry1Ab or ^{125}I-Cry1Ac alone or in the presence of 100-fold mass excess of CR12-MPED, which was the highest toxin:peptide ratio used in bioassays, for 2 h at room temperature. The ^{125}I-labeled toxins bound to BBMV were detected by autoradiography at −80°C for 3 days.

Biosensor Surface Plasmon Resonance Analysis. Surface plasmon resonance measurements were performed by using a BIAcore 3000 system and sensor chip NTA (Biacore, Piscataway, NJ). Hepes buffered saline-P20 (0.01 M Hepes/0.15 M NaCl/0.005% surfactant P20, pH 7.4) was used as running buffer. The ligands, CR12-MPED and CR12-MPED/Del at 10 μg/ml in running buffer, were captured on flow cell 2 at densities of ≈500 response units at a flow rate of 5 μl/min. The analyte (Cry1Ab toxin) was injected over flow cells 1 and 2 at a flow rate of 30 μl/min. The complex was allowed to associate and dissociate for 120 s and 180 s, respectively. The surface was regenerated with an 80-μl injection of 0.01 M Hepes/0.15 M NaCl/0.25 M EDTA/0.005% surfactant P20, pH 7.4, followed by a 25-μl injection of 500 μM NiSO4 at a flow rate of 5 μl/min. Various concentrations of toxin (250–2,000 nM) were injected over both flow cells, and the response curve on flow cell 1 was subtracted from flow cell 2. The data were fitted by global analysis with BIAevaluation, version 3.1 software (Biacore).

Histomicroscopy. Insect midguts were dissected from 10-day-old *M. sexta* larvae. Longitudinal sections (3 μm thick) of posterior midgut were prepared as described by Chen *et al.* (7). After blocking, sections were treated with TAMRA-labeled Cry1Ab (0.1 μg/ml), Cry1Ac (0.1 μg/ml), CR12-MPED (2 μg/ml), BSA (2 μg/ml), or the mixture of TAMRA-labeled Cry1A (0.1 μg/ml) with 20-fold (mass) excess of unlabeled CR12-MPED. Immunolocalization of Bt-R_1 in midgut sections was achieved with a polyclonal antiserum against CR12-MPED. Midgut sections were observed, and images were collected as described by Chen *et al.* (7).

We thank Dr. Jeffrey L. Urbauer for assistance in CD and NMR spectroscopy and Dr. Sue MacIntosh and two anonymous individuals for reviewing versions of this manuscript. This research was supported by Cooperative State Research, Education, and Extension Service-U.S. Department of Agriculture-Natural Resources Institute Grant 2004-35607-14936), National Institutes of Health Grant R01 AI 29092, and a research contract from InsectiGen, Inc. (Athens, GA).

1. Brickle DS, Turnipseed SG, Sullivan MJ (2001) *J Econ Entomol* 94:86–92.
2. Bravo A, Gomez I, Conde J, Munoz-Garay C, Sanchez J, Miranda R, Zhuang M, Gill SS, Soberon M (2004) *Biochim Biophys Acta* 1667:38–46.
3. Zhang X, Candas M, Griko NB, Rose-Young L, Bulla LA, Jr (2005) *Cell Death Differ* 12:1407–1416.
4. Broderick NA, Raffa KF, Handelsman J (2006) *Proc Natl Acad Sci USA* 103:15196–15199.
5. Dorsch JA, Candas M, Griko NB, Maaty WSA, Midboe EG, Vadlamudi RK, Bulla LAJ (2002) *Insect Biochem Molec Biol* 32:1025–1036.
6. Carthew RW (2005) *Curr Opin Genet Dev* 15:358–363.
7. Chen J, Brown MR, Hua G, Adang MJ (2005) *Cell Tissue Res* 321:123–129.
8. Keeton TP, Francis BR, Maaty WSA, Bulla J, LA (1998) *Appl Environ Microbiol* 64:2158–2165.
9. Gomez I, Oltean DI, Gill SS, Bravo A, Soberon M (2001) *J Biol Chem* 276:28906–28912.
10. Hua G, Jurat-Fuentes JL, Adang MJ (2004) *J Biol Chem* 279:28051–28056.
11. Flannagan RD, Yu CG, Mathis JP, Meyer TE, Shi X, Siqueira HA, Siegfried BD (2005) *Insect Biochem Molec Biol* 35:33–40.
12. Jurat-Fuentes JL, Adang MJ (2006) *Biochemistry* 45:9688–9695.
13. Jenkins JL, Dean DH (2001) *BMC Biochem* 2:12–19.
14. Gahan LJ, Gould F, Heckel DG (2001) *Science* 293:857–860.
15. Morin S, Biggs RW, Sisteron MS, Shriver L, Ellers-Kirk C, Higginson D, Holley D, Gahan LJ, Heckel DG, Carriere Y, *et al.* (2003) *Proc Natl Acad Sci USA* 100:5004–5009.
16. Xu X, Yu L, Wu Y (2005) *Appl Environ Microbiol* 71:948–954.
17. Candas M, Francis BR, Griko NB, Midboe EG, Bulla LA (2002) *Biochemistry* 41:13717–13724.
18. Ali MI, Luttrell RG, Young SY, 3rd (2006) *J Econ Entomol* 99:164–175.
19. Luttrell RG, Wan L, Knighten K (1999) *J Econ Entomol* 92:21–32.
20. Xie R, Zhuang M, Ross LS, Gomez I, Oltean DI, Bravo A, Soberon M, Gill SS (2005) *J Biol Chem* 280:8416–8425.
21. Knight PJK, Crickmore N, Ellar DJ (1994) *Molec Microbiol* 11:429–436.
22. Sangadala S, Walters FS, English LH, Adang MJ (1994) *J Biol Chem* 269:10088–10092.
23. Knight PJK, Knowles BH, Ellar DJ (1995) *J Biol Chem* 270:17765–17770.
24. Jurat-Fuentes JL, Adang MJ (2004) *Eur J Biochem* 271:3127–3135.
25. McNall RJ, Adang MJ (2003) *Insect Biochem Molec Biol* 33:999–1010.
26. Griffitts JS, Haslam SM, Yang T, Garczynski SF, Mulloy B, Morris H, Cremer PS, Dell A, Adang MJ, Aroian RV (2005) *Science* 307:922–925.
27. Pardo-Lopez L, Gomez I, Rausell C, Sanchez J, Soberon M, Bravo A (2006) *Biochemistry* 45:10329–10336.
28. Tabashnik B (1992) *Appl Environ Microbiol* 58:3343–3346.
29. Tabashnik BE (1994) *Annu Rev Entomol* 39:47–79.
30. Lee MK, Curtiss A, Alcantara E, Dean DH (1996) *Appl Environ Microbiol* 62(2):583–586.
31. Perez C, Fernandez LE, Sun J, Folch JL, Gill SS, Soberon M, Bravo A (2005) *Proc Natl Acad Sci USA* 102:18303–18308.
32. Regev A, Keller M, Strizhov N, Sneh B, Prudovsky E, Chet I, Ginzberg I, Koncz-Kalman Z, Koncz C, Schell J, *et al.* (1996) *Appl Environ Microbiol* 62:3581–3586.
33. Granados RR, Fu Y, Corsaro B, Hughes PR (2001) *Biological Control* 20:153–159.
34. Federici BA, Park HW, Bideshi DK, Wirth MC, Johnson JJ (2003) *J Exp Biol* 206:3877–3885.
35. Luo K, Banks D, Adang MJ (1999) *Appl Environ Microbiol* 65:457–464.
36. Bradford M (1976) *Anal Biochem* 72:248–254.
37. Hua G, Jurat-Fuentes JL, Adang MJ (2004) *Insect Biochem Molec Biol* 34:193–202.
38. Lobley A, Whitmore L, Wallace BA (2002) *Bioinformatics* 18:211–212.
39. Whitmore L, Wallace BA (2004) *Nucleic Acids Res* 32:W668–W673.
40. Garczynski SF, Crim JW, Adang MJ (1991) *Appl Environ Microbiol* 57:2816–2820.
41. Banks DJ, Hua G, Adang MJ (2003) *Insect Biochem Molec Biol* 33:499–508.
42. Wolfersberger MG, Luthy P, Maurer A, Parenti P, Sacchi VF, Giordana B, Hanozet GM (1987) *Comp Biochem Physiol A* 86:301–308.